How Sustainable is Cable Blowing?

W. Griffioen[1], G. Martel[1], T. Martin[1], R. Lobstein[1], M. van Moppes[2]

[1]Plumettaz, Bex, Switzerland, +31-620209745 · willem.griffioen@plumettaz.com

[2]HMS machines, Gouda, Netherlands, +31-630203648 · michael.vanmoppes@plumettaz.com

Abstract

Cable blowing is efficient for installing cables into ducts. However, energy consumption of blowing is higher than for pulling, caused by the air flowing much faster than the cable. That's why big air compressors are required to blow optical cables, while much larger power cables are pulled with battery powered E-winches. It is found that energy consumption of blowing can be reduced considerably when air pressure is controlled to the need, making it comparable to pulling or better. Battery-operated compressors or gas bottles can then be used for cable blowing. Tests are done with a blowing machine with automated pressure control.

Keywords: Cable; duct; installation; blowing; sustainable, flow.

1. Introduction

Cable blowing is an efficient way to install cables into ducts. Blowing lengths are longer than for pulling, it is fast, all equipment and labor is at one side of the duct and no extra steps, like installing winch ropes, are required. Therefore, production is high and traffic is avoided, a plus for sustainability. Nevertheless, the sec energy consumption of blowing is high, caused by the fact that air flows much faster than the cable, resulting in the majority of energy wasted in heat. Moreover, in the empty part of the duct in front of the cable all airflow energy is lost. That's why already big air compressors are required to blow optical cables with diameter of around 30 mm, while much larger power cables are pulled with battery powered E-winches. Purpose of this study is reduction of energy to blow cables.

Figure 1. Example of battery operated 3 tons E-winch

Figure 2. Example of 16 kW compressor for cable blowing

2. Calculations

Calculations of (net) energy consumption are done for pulling and for blowing using a numerical example.

2.1 Example

In this study energy consumption is calculated for different scenarios. This is done for an example with a typical microduct cable with diameter D_c of 8 mm, linear weight density w of 0.6 N/m and stiffness EI of 0.5 Nm^2, having a coefficient of friction (COF) f of 0.08 with the 16/12 mm microduct (D_d = 12 mm), in which it is installed over a length L of 1500 m. A continuous approximation of this microduct in an IEC trajectory [1] (180° bend, radius R of 50 x duct ID = 0.6 m each 100 m) is made by duct undulations with amplitude A of 4.16 mm and period P of 1.315 m (taking into account capstan effect and friction from cable stiffness, see Appendix A). Only net force and energy are calculated, ignoring losses other than friction with microduct.

2.2 Pulling

If the cable was pulled in a completely straight microduct and the pay-off force is zero the pulling force F as a function of installed length x follows from [2]:

$$F = fwx \tag{1}$$

At the end of the 1500 m long duct this would be 72 N. The required energy E is found by integrating the force over x:

$$E = \tfrac{1}{2} fwx^2 \tag{2}$$

The total energy required to reach the end of the 1500 m long duct is then 54 kJ. Unfortunately, the duct is never straight and undulations in the duct (in this model the bends are approached by continuous undulations) will give a force F [2,3]:

$$F = wR_u \sinh\left[\frac{f}{R_u}x + \sinh^{-1}\left(\frac{F_0}{wR_u} + \frac{w_B}{w}\right)\right] - w_B R_u \tag{3}$$

With the effective bend radius R_u of the undulations and the cable stiffness contribution w_B given by [3]:

$$R_u = \frac{P^2}{8\pi A} \qquad w_B = \frac{3AEI}{2(P/4)^4} \tag{3a}$$

For the treated example the pulling force F as a function of x is given in Fig. 3, with at the end a force of 516 N (a grey line for the straight duct is also shown). The cumulative (net) energy E follows by integrating eq. (3) over x (formula not given here) resulting in the plot of Fig. 4, with at the end a total (net) energy of 200 kJ (a grey line for the straight duct is also shown).

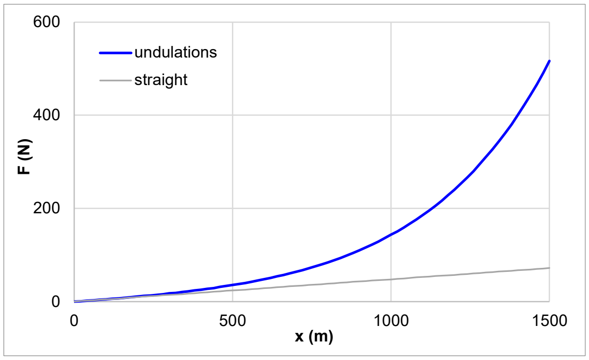

Figure 3. Force *F* to pull the cable as a function of installed length *x*

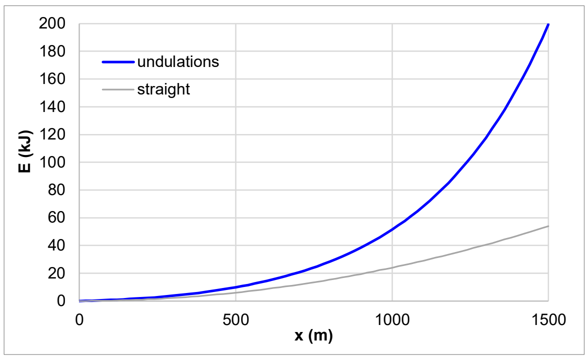

Figure 4. Cumulative (net) energy *E* to pull the cable as a function of installed length *x*

2.3 Blowing

The forces needed to blow a cable in a duct with undulations are lower than those used for pulling. This is because the blowing forces are distributed over the length of the cable, compensating friction locally, so the capstan effect is suppressed. The blowing force consists of 2 parts, the hydrostatic part F_{hs} from the pressure drop over the cable volume eq. (4a) and the hydrodynamic part F_{hd} from the viscous forces exerted on the cable eq. (4b):

$$F_{hs} = \tfrac{1}{4}\pi D_c^2 \Delta p \tag{4a}$$

$$F_{hd} = \tfrac{1}{4}\pi D_c \left(D_d - D_c\right) \Delta p \tag{4b}$$

In fact the hydrostatic part is not supplied by the airflow, but comes from mechanically pushing or pulling the cable into the pressure zone. So, over an installation length L the energy needed is obtained by multiplying the hydrodynamic blowing force with L:

$$E = \tfrac{1}{4}\pi D_c \left(D_d - D_c\right) L \Delta p \tag{5}$$

For the treated example with a pressure of 16 bar the sec blowing energy from the airflow on the cable over the length of 1500 m is then 60 kJ. This can be done easily with 16 bar, also with the undulations in the duct (the required pressure is treated further in this paper) and is already much less than for pulling in that case.

However, blowing uses much more energy than is transferred to the cable, mainly because the air speed is much higher than that of the cable. The speed v_{air} of the air when compressed air is fed through a duct (still no cable) follows with Blasius' law from the applied pressure, the air properties and the geometry [4]:

$$v_{air} = 2.9 \frac{D_d^{5/7}}{\mu^{1/7}\rho^{3/7}} \left(\frac{p_i^2 - p_a^2}{2Lp_a} \right)^{4/7} \tag{6}$$

Here μ is the dynamic viscosity (1.8x10^{-5} Pas) and ρ the density (1.3 kg/m^3) of air and L length of the duct. The applied pressure p_i and pressure at the end p_a need to be taken absolute (not relative to atmospheric). When a pressure of 16 bar (p_i = 17 bar) is fed to the microduct of the example the speed of the airflow will be 98.8 m/s (5930 m/min). That is much faster than the speed of the cable (even when this is 100 m/min). So, a lot of energy is wasted!

The power Π used by the airflow is equal to the product of the speed, cross-sectional area of the inner duct and the pressure:

$$\Pi = 2.3 \frac{D_d^{19/7}}{\mu^{1/7}\rho^{3/7}} \left(\frac{p_i^2 - p_a^2}{2Lp_a} \right)^{4/7} \left(p_i - p_a\right) \tag{7}$$

To maintain 16 bar air pressure over the still empty microduct a power of 18.1 kW would be needed. Blowing with 100 m/min would take 15 minutes and then 16.3 MJ energy, much more than for pulling! This low efficiency is caused by the fact that the airflow is almost 60 times faster than the speed of the cable, i.e. most energy is lost in just flowing the air (and in the empty part of the duct).

Fortunately, the airflow decreases during installation of the cable because the part of the duct filled with cable has a higher pneumatic resistance. This can be described by replacing the duct inner diameter D_d in eq. (6) by the hydraulic diameter D_h. A good match with blowing practice is obtained when using the elliptic definition [5]:

$$D_h = \frac{2\left(D_d - D_c\right)}{1 + \sqrt{\dfrac{D_d - D_c}{D_d + D_c}}} \tag{8}$$

The pressure profile and flow through the duct when partly filled with cable can then be found by equalizing the flow in the filled and the empty part [6]. Using this the following formula is found for the speed v as a function of installed cable length x:

$$v = 2.9 \frac{D_h^{5/7}}{\mu^{1/7}\rho^{3/7}} \left\{ \frac{D_d^{19/4}\left(p_i^2 - p_a^2\right)}{2\left[\left(L - x\right)\left(D_d^2 - D_c^2\right)^{7/4} D_h^{5/4} + x D_d^{19/4}\right] p_a} \right\}^{4/7} \tag{9}$$

The power Π used by the airflow follows again from the product of the speed, cross-sectional area of the inner duct and the pressure. For the treated example then the plot of Fig. 5 follows.

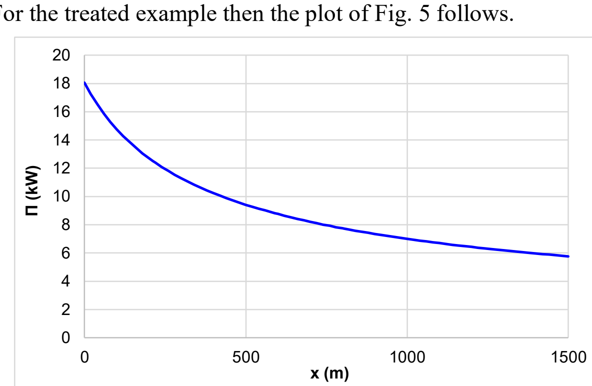

Figure 5. Power *Π* used by the airflow as a function of installed length *x*

Now the power drops from 18.1 kW to 5.8 kW when the cable reaches the end. The total (net) energy is found by integrating the power over the time (formula not given here), for a constant speed of 100 m/min resulting in a total (net) energy of 7 MJ (compared to 16.3 MJ without the filling effect).

It is clear that blowing uses much more energy than pulling. But, blowing is also more efficient. This means that 1500 m can be easily installed for this example, i.e. with lower settings. When a pushing force of 120 N is applied a pressure of 5.52 bar is already sufficient (calculated with JetPlanner 4.0 [7]). A lower pushing force would result in higher pressure needed, so this would lead to more total energy consumption. The 120 N is chosen as a workable pushing force for small blowing machines (and this cable will survive the crashtest). With 5.52 bar the total blowing energy would drop to 793 kJ, see Fig. 6. This is much less than the 7 MJ in the same plot for 16 bar, but still more than the energy of 200 kJ for pulling the cable. The energy for the 120 N pushing can be ignored with respect to the energy required for pulling with 516 N or pure blowing with 5.52 bar (see further).

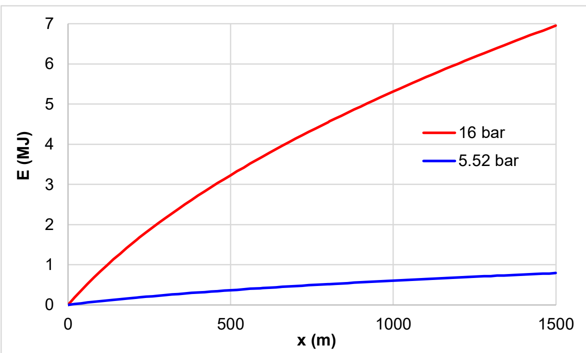

Figure 6. Energy *E* used by the airflow as a function of installed length *x* for 16 bar and 5.52 bar air pressure

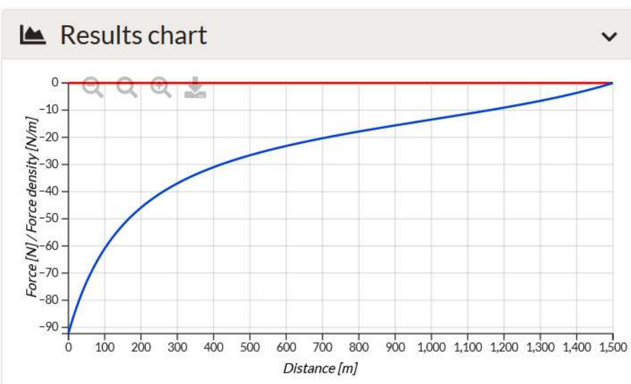

Figure 7. JetPlanner 4.0 result for blowing with 5.52 bar air pressure and 120 N pushing force

We can optimize further, by first installing the cable with pure pushing and then start the compressor when the pushing force becomes too high. For the reach of the pushing force no analytical solution is possible and a numerical simulation must be made. For this again JetPlanner 4.0 is used. It can then be calculated that pushing with 120 N for the numerical example can be done over the first 804 m. This is also the part where more than half of the energy (521 kJ, from Fig. 6) was used by the compressed air. Subtracted from 793 kJ only 272 kJ is left. Already less than for pulling.

This was only with opening the full (required) pressure after pure pushing. But, when increasing the pressure only until the value needed still more can be saved. For this again numerical calculation is needed with JetPlanner 4.0, for the numerical example resulting in the pressure plot of Fig. 8. Calculation is also done for a microduct with D_d of 10 mm.

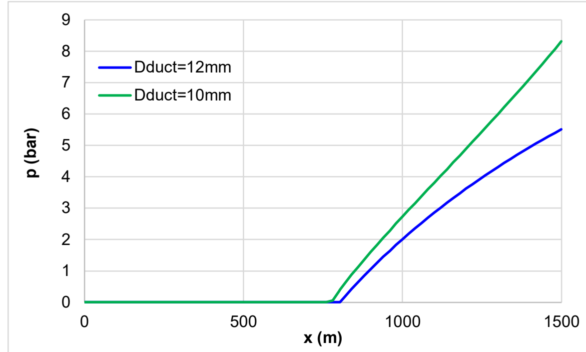

Figure 8. Air pressure *p* required to blow *x* m with microduct open at 1500 m

If then the pressure of Fig. 8 is integrated over x and divided by the speed v_{cab} of 100 m/min then the cumulative energy consumption E of Fig. 9 follows. The end is reached now with only 123 kJ. Now the energy is amply less than the 200 kJ for pulling the same distance!

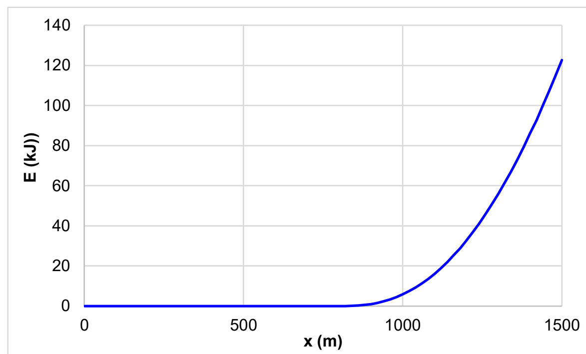

Figure 9. Cumulative (net) energy *E* required to blow *x* m with 5.52 bar and microduct open at 1500 m

Let's check that the energy for pushing can still be neglected. For the pushing force build-up again a simulation by JetPlanner 4.0 is used. In Fig. 10 this pushing force F_{push} is plotted. Note the grey line, which is the part of the total pushing force required to push the cable into the pressure zone, the backpressure force. This part is not contributing anymore to pushing inside the microduct and is in fact supplying the (distributed) hydrostatic part of the blowing force.

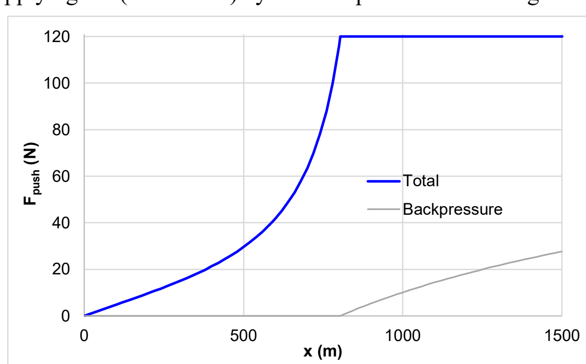

Figure 10. Pushing force F_{push} required to blow *x* m with microduct open at 1500 m

Integrated over the length a total (net) energy for this pushing follows of 109 kJ, see Fig. 11. This cannot be totally ignored anymore, but it is the lowest contribution to the total net power. In total (pushing + blowing) the net energy consumption is 232 kJ, just a bit more than for pulling. Often 8 mm cables are blown into 12/9.8 mm microducts (less airflow), where blowing this way becomes far more energy efficient than pulling.

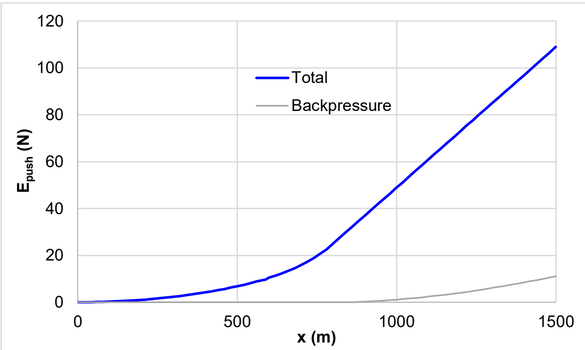

Figure 11. Cumulative (net) energy E_{push} required to blow *x* m with microduct open at 1500 m

3. Unplugged Power Sources

Two different power sources which do not need to be plugged into the mains or a fuel driven aggregator (cord less) and do not require a combustion motor at all are discussed here as options.

3.1 Batteries

Figure 12. Example of too small and too large (for use with energy optimized blowing machines) battery-operated compressor

An electrically driven blowing machine with automatic pressure control makes possible to work entirely with batteries (e.g. two batteries 6.0 Ah – 18 V can store 778 kJ), even for the compressor. There are many small battery-operated compressors for tire inflation on the market. They are sometimes supplying enough pressure and volume flow to be used for blowing, but operation longer than 1 minute is rare (and the batteries are 3 times or more too small). One battery operated compressor suitable for blowing for longer time exist, see Fig. 12, but is large enough to blow cables without any energy optimization. There is a market for an in between battery-operated compressor.

3.2 Gas bottles

An alternative of using a battery operated compressor and still using stored energy (no combustion engine or plug-in required) is using bottles with compressed gas. The volume of gas needed for the treated example, is calculated with Fig. 8 and eq. (9). A total of 324 atmospheric liters is found, see Fig. 13. With a gas bottle of 50 liters under a gas pressure of 200 bar then 30 installations can be done (leaving 276 liter to keep the 5.52 bar for the last part)!

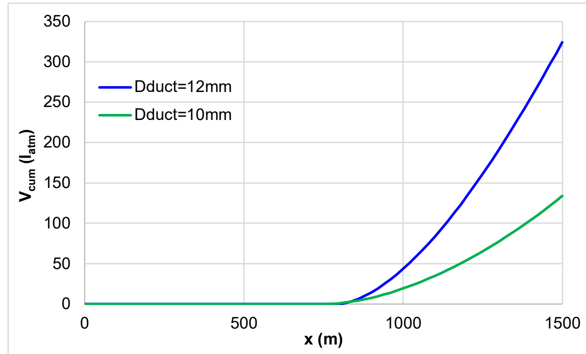

Figure 13. Cumulative volume of air V_{cum} (atmospheric liters) required to blow *x* m until 1500 m

In the treated example the air pressure needed was still low, because of the relatively large microduct diameter. Usually, the maximum cable diameter is used (or when 8 mm is the max cable diameter for the machine, the minimum microduct ID). Let's see what happens when a tight fit with D_d of 10 mm is taken. From Appendix A an amplitude A_d of 2.16 mm and a period P of 0.964 m follows. Now, the pulling force would then increase from 516 N to 621 N. And a higher air pressure of 8.31 bar (see Fig. 8) is needed to reach the end. But, even with this higher pressure the larger pneumatic resistance in the smaller microduct makes the total required air volume decrease to only 134 liter, see Fig. 9. Now 71 installations could be done with one cylinder (leaving 416 liter to keep the 8.31 bar for the last part). So, pulling requires more force (and energy) when the microduct becomes smaller while for blowing the required volume of air (and compressed air energy) gets less.

4. Blowing Tests

Figure 14. Example of battery operated blowing machine with automatic pressure control for optimized blowing

Blowing tests done with the battery-operated blowing machine of Fig. 14 will be treated next. Here already no compressed air is needed for pushing the cable. Test are done with a small electric compressor, but still with a version of the blowing machine without automatic air pressure control. Later, also tests were done with the version with automatic air pressure control. Although battery operated electric compressors of the right size were not yet found, the low air consumption was demonstrated by using gas cylinders as blowing source.

4.1 Test with small electric compressor

Figure 15. Small compressor (right) next to large compressor (left) used earlier

An optical cable with 96 optical fibers and a diameter of 6.5 mm was blown in with the electrically driven blowing machine of Fig. 14 (but not yet with automatic pressure control). It could be installed into a 10/8 mm (max pressure of 16 bar reached) and in a 12/10 mm microduct (7 bar pressure reached and sufficient) of 1200 m long in a 50 m long IEC test track with the small compressor, right in Fig 15, instead of the big compressor used earlier, left in Fig.15.

4.2 Flow tests with pressure controlled machine

Figure 16. Test setup with pressure controled blowing machine and flow measurements, using gas cylinders

The test setup for the tests with the pressure controlled machine is shown in Fig. 16. In the top picture the flow meter is shown on the foreground. It directly measures the flow through the microduct, so no leaks in the system (if present) can disturb the tests. As no cable can be pushed through the flowmeter, the flow is sent through the flowmeter via a bypass unit (black with red connectors). In the bottom picture the gas cylinders used can also be seen.

4.2.1 3.9 mm cable in 10/6 mm microduct. An old (>10 years) cable with 24 optical fibers and a diameter of 3.9 mm was blown into a 10/6 mm microduct in an IEC test track with loops of 50 m long and return (180°) bends with 0.4 m radius, total length about 750 m. No lubricant was used. As this is not an ideal situation the blowing length was not that long, but a good idea was obtained about the air consumption, see Fig. 17. In the top picture it can be seen that the pressure goes up after a certain installed length, to keep the pushing force low. When the max set pressure of 10 bar was reached the pushing force responds by continuously increasing during further installation. After reaching another (higher) pushing force the machine responds in lowering its speed, until the test was stopped at a speed of 10 m/min. The relatively long length installed with a low speed in this tough test track (tougher than the 100 m IEC track used in the theoretical simulations, and usually also tougher than most urban trajectories) is of course not ideal for the air and energy consumption. The total volume of air used (calculated by integrating the flow over time) was 581 liter (atmospheric) while the total net energy used for the compressed air was 521 kJ. The pressure in the gas bottle (50 l) dropped from 190 bar to 170 bar (there were a few air losses in the pneumatic connections). The airflow of the empty microduct with air pressure 10 bar was 92 l/min. If present the total installation time of 17 minutes the energy consumption would have been 1564 kJ.

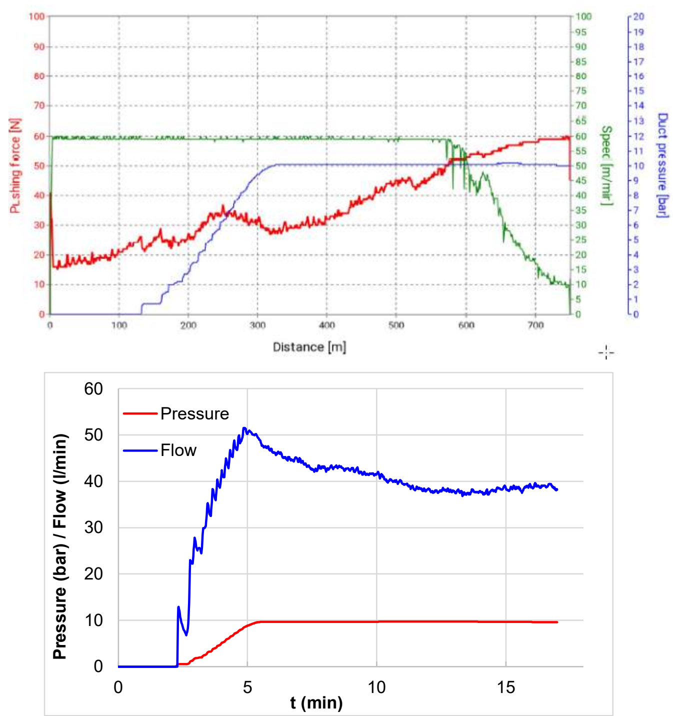

Figure 17. Test with 3.9 mm cable into 750 m of 10/6 mm microduct in 50 m long 180° looped (bend radius 40 cm) IEC test track. Top picture with pushing force, air pressure and speed as a function of distance, bottom picture with air pressure and flow as a function of time.

4.2.2 6.8 mm cable in 10/8 mm microduct. Another old cable with 12 optical fibers (only one of the tubes filled) and a diameter of 6.8 mm was blown into a 10/8 mm microduct in an IEC tests track with loops of 50 m long and return (180°) bends with 0.8 m radius, total length about 957 m. A good idea about the air consumption was obtained from the flow in Fig. 18. The maximum pressure was set at 15 bar. The total volume of air used was 656 liter (atmospheric) while the total net energy used for the compressed air was 830 kJ. The pressure in the gas bottle dropped from 138 bar to 104 bar.

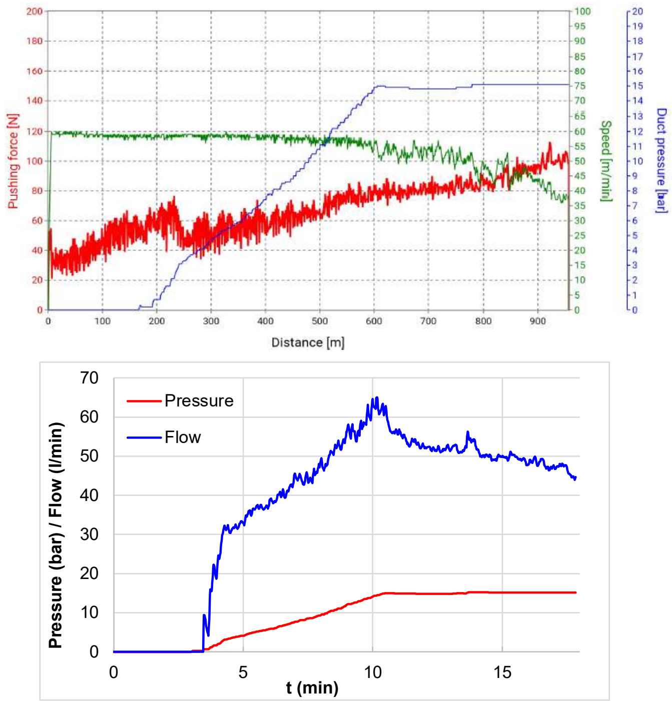

Figure 18. Test with 6.8 mm cable into 957 m of 10/8 mm microduct in 50 m long 180° looped (bend radius 80 cm) IEC test track. Top picture with pushing force, air pressure and speed as a function of distance, bottom picture with air pressure and flow as a function of time.

5. Conclusions

It has been shown theoretically that cable blowing with automatically controlled air pressure can save a lot of energy. The first part can be installed by pushing only. When the air pressure is applied the filling of the duct has already increased the pneumatic resistance, so the air flow, and hence the energy consumption, is less. When the cable is installed further the pressure increases, while at the same time also the pneumatic resistance increases, so the flow remains limited. Blowing tests have been done with 2 different cables in 2 different microducts. The conditions were very tough, much tougher than in the theoretical simulations, and also the speed was relatively low (the speed at the start, but especially at the end), but even then it was shown that a lot of energy was saved. That's why the tests could have been done with gas (nitrogen) bottles as air supply.

6. Acknowledgments

We wish to express our thanks for their different roles in this paper, to Jim Boelsma, Bart Schouten, Bob Muller (Leidsche instrument-makers School, NL), Arjan van Veen, Ewald Sterkenburg, Ronald Gomersbach (HMS-Machines, NL), Hugo Kugler (Farrier, CH), Rolf Ambühl, Nicolas Lebon, Yvan Chappuis, Valery Naula, Damien Plumettaz, Gregory Laurent and David Clement (Plumettaz, CH).

7. References

[1] IEC 60794-1-21, 2015, "Optical Cable Test Procedures", method E24

[2] R.C. Rifenburg, "Pipe-line design for pipe-type feeders", *Transactions AIEE Power Apparatus and Systems*, vol. 72, part III, 1953, pp. 1275-1284

[3] W. Griffioen, H.G. Nobach, G. Plumettaz, "Theory, software, testing and practice of cable in duct installation", *Proc 55th IWCS* (2006) 357-365 and *Trans IWCS*, Vol.1 (2008) 102-110

[4] V.L. Streeter, "*Fluid mechanics*", McGraw-Hill, New York (1957)

[5] W. Griffioen, L. Gapany, S. Grobety, C. Gutberlet, G. Plumettaz, R. van der Sluis, A. Pijpers, Th. Weigel, "Floating Cable into Duct: Recent Developments", *Proc 62nd IWCS* (2013) 11-20

[6] A. Snippe, O. Bresser, S. Hoekstra, W. Griffioen, "Modeling the Pressure Profile for Moving Optical Cables in Ducts", *Proc 62nd IWCS* (2013) 26-34

[7] JetPlanner 4.0: Plumettaz proprietary software to calculate cable in duct installation for different methods, like blowing. www.plumettaz.com/en/service/jetplanner

8. Appendix A: Effective Undulations

A standard trajectory for blowing test is the IEC trajectory [1]. It is made of loops of duct of e.g. 100 m long, connected by 180° bends with e.g. for (standard) microducts a bend radius R of 40 times the outer diameter of the duct, or 50 times the inner diameter D_d of the duct. Analysis of force build-up and energy consumption during cable installation becomes easier when the properties of this trajectory are translated to continuous undulations. Two properties should match, the capstan effect and the friction due to cable stiffness.

The capstan effect is determined by the change of angle $d\beta/dx$ per unit of length. For the IEC with 100 m loop lengths this is:

$$\frac{d\beta}{dx} = \frac{\pi}{100} \tag{A1}$$

For duct undulations with effective amplitude A (duct amplitude A_d, as used in JetPlanner 4.0) and period P this is [3]:

$$\frac{d\beta}{dx} = \frac{8\pi A}{P^2} \quad \text{with} \quad A = A_d - \tfrac{1}{2}\left(D_d - D_c\right) \tag{A2}$$

Here D_c is the cable diameter. From (A1) and (A2) it follows:

$$A = \frac{P^2}{800} \tag{A3}$$

The friction dF_u/dx per unit of length due to cable stiffness in undulations is given by [3]:

$$\frac{dF_u}{dx} = \frac{3EIAf}{2\left(P/4\right)^4} \tag{A4}$$

Here EI is the bending stiffness of the cable and R the bend radius of the duct. The friction F_b due to cable stiffness in bends is given by [3]:

$$F_b = \frac{2EIf}{\sqrt{6\left(D_d - D_c\right)R^3}} \tag{A5}$$

This stiffness friction shall be compared, in SI units, with 100 times the friction per meter of (A4):

$$A = \frac{4(P/4)^4}{300\sqrt{6(D_d - D_c)R^3}} \quad \text{(A6)}$$

From (A3) and (A6) then follows:

$$P^2 = 24\sqrt{6(D_d - D_c)R^3} \quad \text{(A7)}$$

When taking the bend radius R equal to $50D_d$ (is about 40x*OD*) (A7) becomes:

$$P^2 = 12000\sqrt{3(D_d - D_c)D_d^3} \quad \text{(A8)}$$

And with (A3):

$$A = 15\sqrt{3(D_d - D_c)D_d^3} \quad \text{(A9)}$$

Example: D_c = 8 mm and D_d = 12 mm. The IEC trajectory would have bend radii of 0.6 m (50 x D_d). Undulations follow with amplitude A = 2.16 mm and period P = 1.315 m. The duct undulation amplitude A_d (used in JetPlanner 4.0) is then 4.16 mm.

Note that for the lowest forces the IEC trajectory is a bit more severe than the undulation approximation, because the latter adds gravity and capstan/stiffness friction quadratic (because the normal forces point in arbitrary directions). In the IEC trajectory the capstan/stiffness friction is concentrated in the bends and therefore in fact adds linearly. So, the examples treated are about true for an IEC test track with COF of about 0.07 (also a value often achieved).

9. Pictures of Authors

Willem Griffioen received his M.Sc. degree in Physics and Mathematics at Leiden University (NL) 1980, worked there until 1984. Then employed at KPN Research, Leidschendam (NL), on Outside-Plant Installation Techniques. In 1995 he received his Ph.D. (Optical Fiber Reliability) at Eindhoven Techn. University (NL). From 1998 to 2009, he worked at Draka Comteq, Gouda (NL), on Connectivity of FttH. Currently he works at Plumettaz SA, Route de la Gribannaz 7, CH1880 Bex (CH), willem.griffioen@plumettaz.com and is responsible for R&D of cable installation techniques.

Guillaume Martel Holds a MSc. in Mechanical Engineering (INSA-Lyon 1994 - FRA) and an MBA (Ashridge 2005 - UK). With a managerial background in R&D, Manufacturing, Business Development, Operations, and Organisational Development in the Automotive and Industrial Equipment sectors, Guillaume joined Plumettaz in 2022 as Product Manager.

Thomas Martin holds a Master of Science degree in Electronics and Embedded Systems from ISEP in Paris, France (2018). He began his career in the defense industry at Nexter System, where he worked for five years on the design and validation of complex integrated systems, combining electronics, hardware, mechanics, and software. In 2023, he joined Plumettaz SA, where he currently heads the validation department.

Roland Lobstein holds a Master's degree in Mechanical Engineering from INSA Strasbourg, France (2005). Following graduation, he embarked on a career in the automotive industry, focusing on mechatronic systems design and development for over a decade. In 2014, he transitioned his expertise to railway systems engineering at Bombardier Transportation. Since 2018, Roland has been a Project Manager at Plumettaz SA, currently leading the development of their next-generation optical fiber installation machine.

Michael van Moppes received a M.Sc. degree in Material Science and Engineering from Delft University of Technology in 1988. After various function's within the aerospace, aluminium and offshore industry he joined Plumettaz b.v. (NL) in 1998 as Area Sales Manager responsible for Northern and Western Europe. From 2005 he has been responsible for APAC region and in 2009 became Vice-General Manager at Plumettaz Project Equipment (Shanghai) Co., Ltd. In 2011 he became General Manager at Plumettaz Singapore Pte. Ltd., and December 2020 he joined H.M.S. Machines, Gouda, The Netherlands as Application Manager Plumettaz Group.